# WATER AND AQUEOUS SOLUTIONS AT HIGH PRESSURES AND TEMPERATURES

E. U. Franck

*Institut für Physikalische Chemie, Universität Karlsruhe,
Karlsruhe, Germany*

## ABSTRACT

A survey is given of recent results on properties of water and aqueous solutions at high pressures and high temperatures with emphasis on supercritical conditions. New *PVT*-data for water from static measurements are available to 1 000°C and 10 kb. Dielectric constants and viscosity have been measured to 550°C and 5 kb. Infra-red and Raman spectra of OD-vibrations of HDO in $H_2O$ to 400°C and 5 kb give information about the extent of hydrogen bonded structure. Critical curves of binary aqueous systems with one inert component, for example argon, extending to 3 kb and 400°C are discussed. Absorption spectra of bivalent cobalt and nickel chlorides are measured to 500°C and 6 kb and conclusions about the stability of octahedral and tetra-hedral complexes are drawn. Shock wave and static conductance measurements to 1 000°C and more than 100 kb demonstrate the increase of the ion product of water by twelve orders of magnitude or more at these conditions.

## I. INTRODUCTION

WATER and aqueous solutions are, very probably, the most thoroughly investigated class of fluids. An extraordinary amount of information is available for moderate temperatures and for pressures close to the normal vapour pressures. The knowledge of such fluids at temperatures approaching and exceeding the critical temperature of water, however, is much more limited. This is particularly true for those properties which are of interest for chemistry, as for example the electrolytic behaviour of water, solubility and miscibility at high temperatures and chemical equilibria at supercritical conditions. In recent years, work in this field has increased considerably, however, partly as a consequence of the advent of many new strong and non-corrosive construction materials. A survey of some selected results of this new work will be presented.

As an introduction a temperature/density diagram for pure water is given in *Figure 1*. The non-shaded area is the range of existence for a homogeneous fluid. At density 1 g/cm³, near the abscissa is the triple point (T.P.). The points on the heavy (dashed) line extending to the right denote the transitions between the different modifications of ice. A number of isobars are shown. Up to about 10 kb data from static experiments for the density of water are available from recent work[1-3]. At pressures above about 25 kb, water densities at high temperatures have been derived from shock wave experiments[4].

The intermediate range has to be covered by interpolation. In order to retain the normal density at 1 g/cm³ to 500°C a pressure of about 8 kb is necessary. At 1000°C pressures of about 20 kb have to be applied for the same purpose.
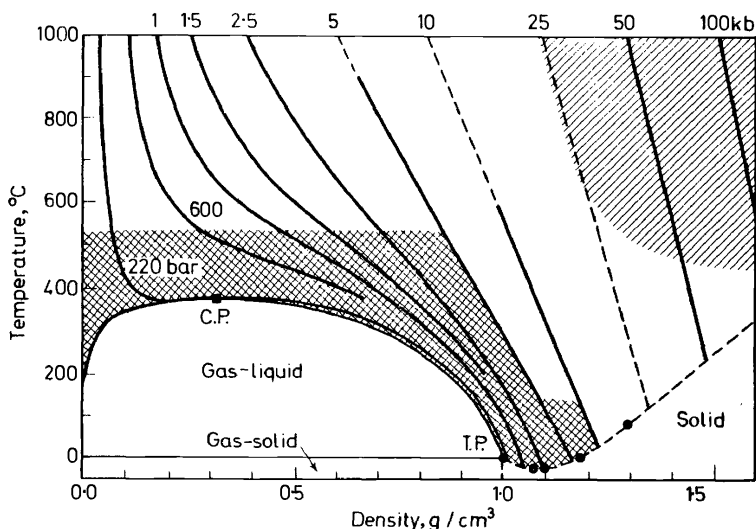


*Figure 1.* Temperature/density diagram of water. Full lines: measured isobars. Dashed lines: interpolated isobars. Cross-hatched zone: viscosity and dielectric constants determined. Single shading: ionic conductance determined.

In order to evaluate the possibilities of water at high pressures and elevated temperatures as a chemical solvent, knowledge of the dielectric constant and of the viscosity are particularly useful. The cross-hatched area up to about 500°C and 5 kb in *Figure 1* denotes the conditions at which the static dielectric constant[5] and the viscosity[5, 6] have been determined experimentally. At supercritical temperatures, for example at 500°C, the viscosity varies much less with the density of the fluid than at low temperatures. At 0·2 g/cm³ and 0·8 g/cm³ and at 500°C the viscosity has been found to be 3·8 × 10⁻⁴ poise (P) and 10·5 × 10⁻⁴ P respectively. This means that the viscosity is lower than that of liquid water at room temperature by a factor of 10 or 20. Dense supercritical water is a medium of very high fluidity and, consequently, dissolved neutral or ionic particles have high diffusion coefficients and ion mobilities in this medium.

In the upper right part of *Figure 1* the region has been approximately indicated in which direct determinations of the conductance and ionic product of water have been made with shock wave and static experiments. It appears as if at 1000°C and pressures beyond 100 kb water approaches the state of an ionic fluid.

## II. DIELECTRIC AND SPECTROSCOPIC PROPERTIES

The static dielectric constant of water is to a large extent determined by the

peculiar structural properties caused by the hydrogen bonds. In order to calculate the dielectric constant, the equation of Kirkwood[7, 8] introduces a correlation parameter which is determined by the number and orientation of the nearest neighbours of each water molecule. This approach gave good results at low temperatures. It is interesting to investigate the correlation parameter for supercritical water.

Earlier measurements of the dielectric constant at elevated temperatures were made up to 400°C and in part to 2 kb (for a compilation see Quist and Marshall[9]). Only recently experimental determinations were performed to 550°C and 5 kb[10]. The capacity of a condenser made of gold–palladium half cylinders mounted inside a high pressure autoclave was determined at a frequency of 1 MHz. One of the half cylinders could be rotated at high temperatures and pressures. *Figure 2* gives a compilation of results as curves of dielectric constants superimposed on the isobars of a temperature/density diagram of water. At supercritical temperatures and high pressure, values of the constant between 5 and 25 can be obtained. This corresponds to the dielectric properties of polar organic liquids under normal conditions.
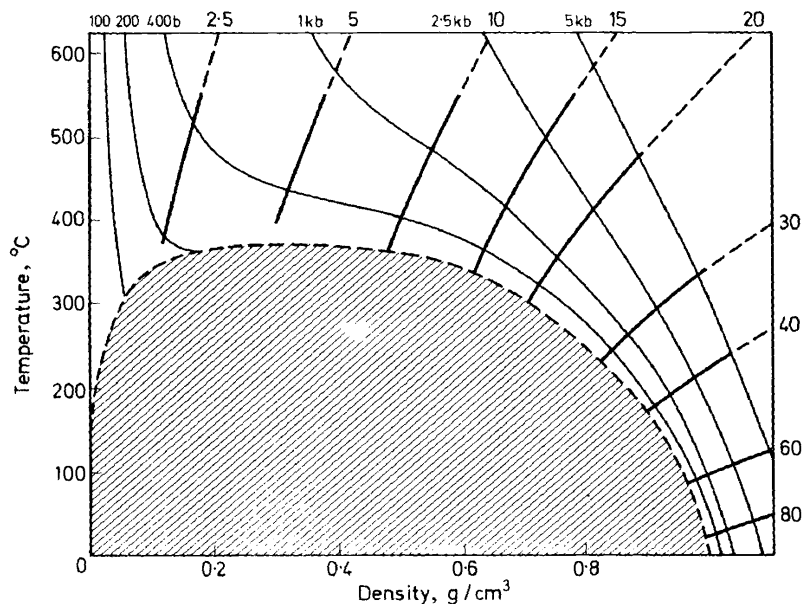


*Figure 2.* Dielectric constant of water as a function of temperature and density. ——: Measured. — — —: Calculated. ——: Isobars.

The new experimental data permit the calculation of the correlation parameter $g$ according to the Kirkwood equation which is inserted in *Figure 3*. *Figure 3* gives such values of $g$ obtained as a function of water density for several temperatures. As is expected, the $g$-values approach unity with decreasing density. It is interesting that even at 400°C and around the critical density of 0·32 g/cm$^3$ the $g$-parameter is still about 1·5 or 1·6, which
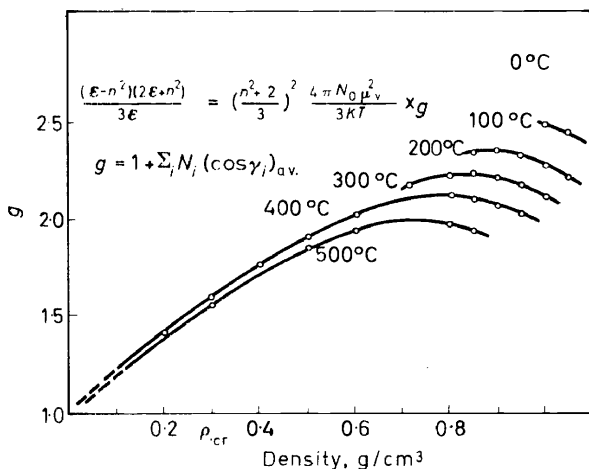
*Figure 3.* The Kirkwood correlation parameter from the experimental dielectric constant $\varepsilon$ of water as a function of density and temperature (For a discussion of the inserted equation see ref. 8).

may indicate that a certain amount of structure still exists under these conditions. For a detailed discussion see ref. 8. It would be desirable to investigate dense supercritical hydrogen chloride in the same way for comparison.

More detailed information about the association of water by hydrogen bonds can be expected from the infra-red absorption spectrum. Particularly well suited for this purpose is the study of the absorption of the OD-vibration around $2500$ cm$^{-1}$ of HDO diluted in H$_2$O because of the absence of inter-
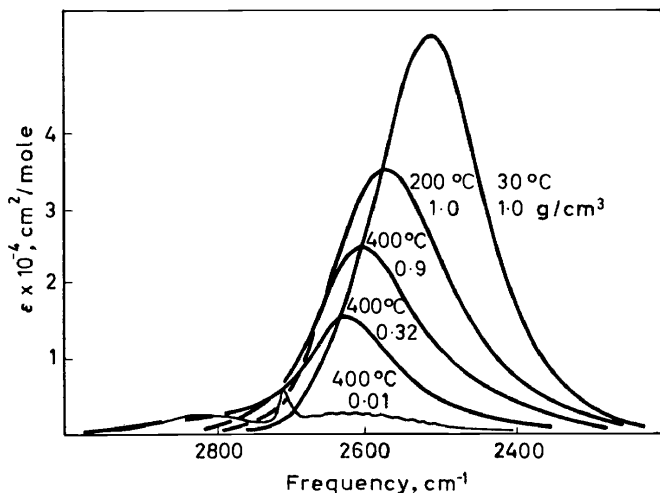


*Figure 4.* Infra-red OD absorption bands of 9·5 mole per cent HDO in H$_2$O for different temperatures and densities.

16

ference of other vibrations in this frequency range. Thus the HDO-absorption has recently been measured up to 500°C and partly up to 4 kb[12]. A special absorption cell of the reflection type, similar in some respects to a cell described by Welsh et al.[13], had been designed for the purpose. It has a single window of colourless synthetic sapphire with a platinum–iridium mirror close to its inner surface. Figure 4 gives a selected number of absorption bands.

Three of these bands at 30°, 200° and 400°C have been obtained at or almost at the normal liquid density of 1 g/cm³. The high absorption intensity at room temperature, which is considered to be caused by the hydrogen bonded structure of the liquid, decreases with temperature but remains relatively high. The frequency of the maximum shifts from $2507$ cm$^{-1}$ to slightly over $2600$ cm$^{-1}$ at 400°C and 0·9 g cm³. $2720$ cm$^{-1}$ is the value for the $Q$-branch of this vibration in dilute HDO-gas. The bands, however, become increasingly asymmetric, although a shoulder on the low frequency side is not visible. At a constant temperature of 400°C the rotational structure of the vibrational band appears only at densities below 0·1 g/cm³. This means that even at the supercritical temperature of 400°C and at densities between 0·1 and 1·0 g/cm³ very considerable intermolecular interaction and possibly association must exist, which may be partly caused by hydrogen bonding.
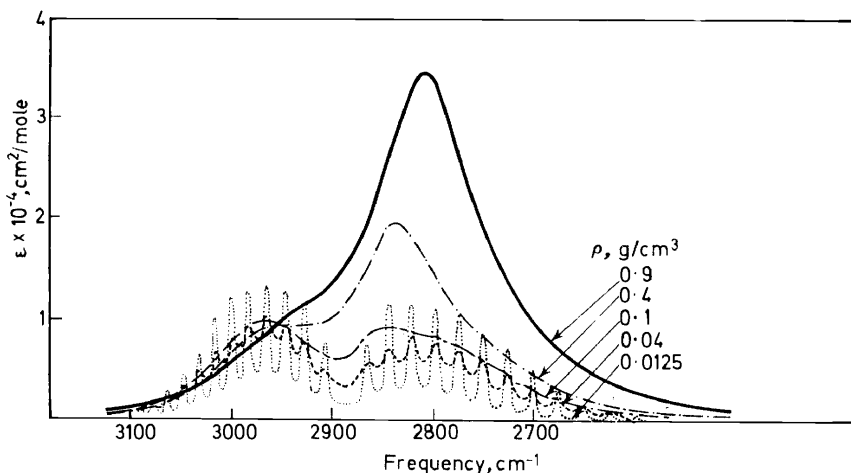


Figure 5. Infra-red absorption of HCl at 150°C for different densities $\rho$.

For comparison, Figure 5 gives the infra-red absorption of compressed supercritical hydrogen chloride at several densities[14]. Although lower in intensity the absorption of the highest density of 0·9 g/cm³ is not very different in appearance from that of HDO. In both cases decreasing density causes a shift of the maximum frequency towards higher values. This behaviour is demonstrated in Figure 6, where the frequency shift isotherms for both compounds have been plotted as a function of the reduced density. Below 400°C the frequency shifts for HDO have a pronounced temperature dependence, while above 400°C the behaviour of the frequency shifts for
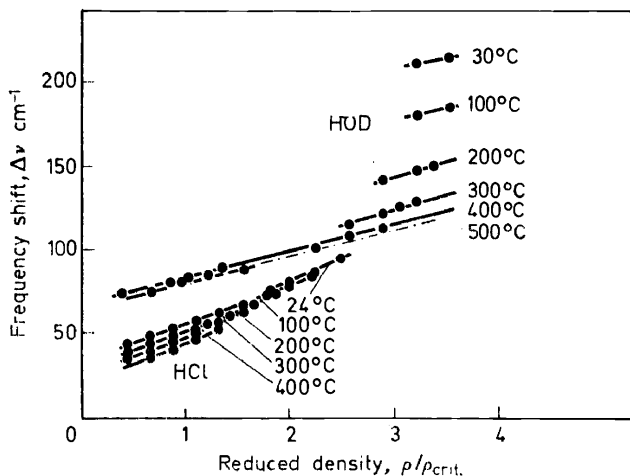
17

*Figure 6.* Frequency shift $\Delta v = v_{gas} - v_{max}$ of HCl- and OD-vibrations.

HDO and HCl appear to become more alike, suggesting that dipole interactions other than those leading to hydrogen bonds become dominating in dense water above about 400°C.

It is possible that the Raman spectrum of HDO diluted in normal water reveals more information about the hydrogen-bonded structure than does infra-red absorption. In *Figure 7* Raman scattering curves are given[15] for temperatures to 400°C and densities between 0·1 and 1·0 g/cm³. The curve for 25°C clearly shows a shoulder at about 2650 cm⁻¹ which has already been observed by other authors[16]. If the temperature is increased at almost constant high density to 400°C, a new band seems to appear at the position of this shoulder. Considering the evidence and discussion of Walrafen[16] and other authors[8], one might take this 2650 cm⁻¹ band as an indication for water molecules which are not hydrogen bonded, but which nevertheless interact strongly with each other. Decrease of density to 0·1 g/cm³ at 400°C
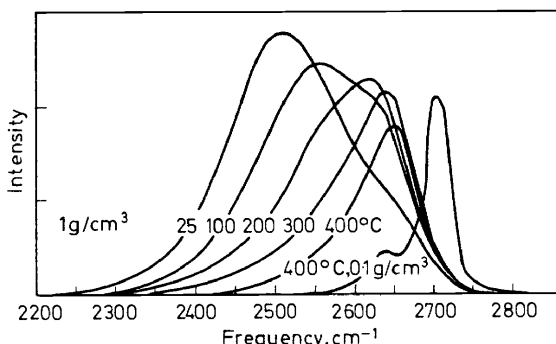


*Figure 7.* Raman intensity of the OD-vibration of HDO. (6·2 mole/l. $D_2O$ in $H_2O$; slit width: 18 cm⁻¹; argon laser, 4 880 Å).
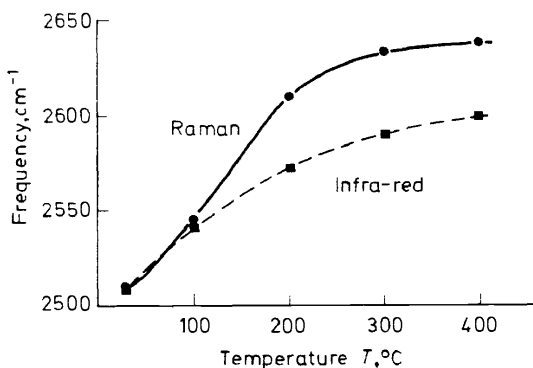
18

*Figure 8.* Frequency shift of OD-vibration of HDO in H$_2$O with temperature at constant density of 1·0 g/cm$^3$.

this band considerably changes. A detailed analysis of numerous spectra at densities from 1·0 to 0·015 g/cm$^3$ has been made. It shows that the band which appears as a shoulder at 2650 cm$^{-1}$ gradually transforms into a sharp peak at 2710 cm$^{-1}$ at 400°C and very low density. It is possible that this band indicates non-hydrogen-bonded OD-groups.

The frequency shifts of the maxima discussed above are shown for a constant density of 1 g/cm$^3$ as a function of temperature in *Figure 8.* Below 100°C the infra-red and Raman curves almost coincide. Above that temperature the Raman shifts are higher and the shape of the curve is different. This may be due to the fact that the Raman curve in *Figure 8* actually combines the frequency shifts of the '2507-band' at low temperature with those of the '2650-band' at high temperature. In the infra-red, the absorption of hydrogen bonded OD-groups around 2507 cm$^{-1}$ and more may be so much stronger than a possible absorption around 2650 cm$^{-1}$ that this latter is not clearly observed.

## III. ABSORPTION SPECTRA OF DISSOLVED COMPLEXES

Spectroscopic evidence is also available for the association of water molecules with dissolved ions and complexes at high temperature and high pressure. Several heavy metals can form complex compounds which are stable enough to exist in aqueous fluids even at supercritical temperatures. In some cases the stability of such complexes can be increased by the addition of high concentrations of alkali halides to the fluid. Such 'hydrothermal' solutions are of importance as transport media for heavy metals within certain areas of the earth's crust[17].

Recently the range of existence of complexes of bivalent cobalt and nickel has been investigated spectroscopically in the visible and near-ultra-violet regions[18, 19, 20]. For this purpose absorption double cells were designed and built, which could be used with aqueous solutions to 500°C and 6 kbar. The windows were cylindrical rods of synthetic colourless sapphire of 60 mm length. The high temperature inside the cells decreases along the length of

19

these windows. The cells were of a non-corrosive high strength alloy and in some cases lined with gold–palladium or platinum.

Dilute solutions of bivalent cobalt chloride were investigated to 500°C. The pink solution at 25°C has a maximum of absorption at 515 nm. At 300°C and the relatively low pressure of 350 bar a blue solution with a much
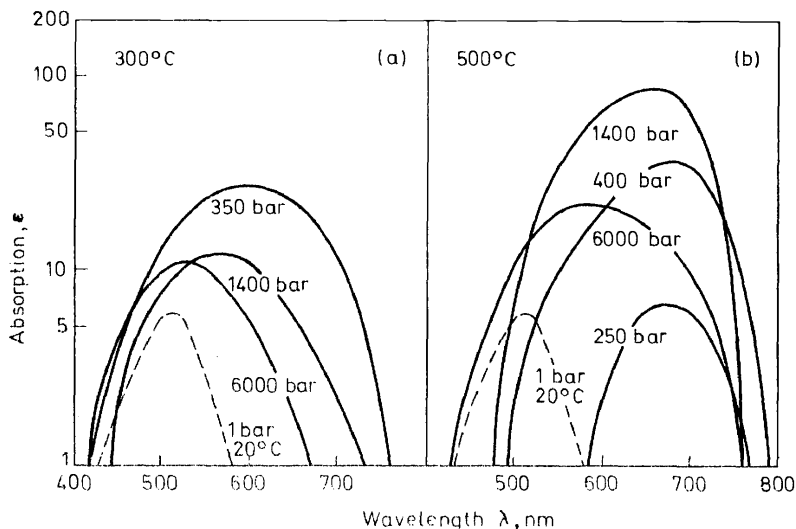


*Figure 9.* Absorption spectrum of CoCl$_2$ in water (Molality: 0·01) at (a) 300°C and (b) 500°C between 250 and 6000 bar.

stronger absorption having a maximum around 600 nm is formed. Increasing the pressure to 6 kb reduces the absorption and shifts the maximum to about 520 nm [*Figure 9*(a)]. This shift in absorption is explained by assuming an equilibrium between bivalent positively charged hexaquocobalt complexes, absorbing at shorter wavelengths and neutral dichlorodiaquocobalt complexes. The first have an octahedral and the second a tetrahedral structure. Increase of temperature favours the lower coordinated complex with four ligands, increase of pressure favours the higher coordinated complex with six ligands. This is even more obvious at 500°C [*Figure 9*(b)]. At 1400 bar the tetrahedral complexes with their strong absorption predominate. A pressure of 6 kb cannot shift the equilibrium towards the octahedral structure to the same extent as at 300°C. It is suggested that the reduction of absorption caused by a pressure decrease to 250 bar indicates a growing proportion of only slightly hydrated cobalt chloride molecules which are known to exist in the gas phase at high temperatures even without the presence of water.

Similar observations can be made with nickel(II) chloride if a high concentration of chloride ion is added. *Figure 10* gives absorption curves at 300°C in 4-molal sodium chloride solution as examples. The curve for 25°C corresponds to the light green normal solution with two absorbing electron transitions. Temperature increase to 300°C produces blue solutions with a

20

strong broad band at 680 nm. It is caused by a combination of bands from octahedral and tetrahedral complexes. The tetrahedral complexes appear to predominate. Additional spectra indicate that this kind of complex becomes the only stable form in 10-molal lithium chloride solutions at this temperature
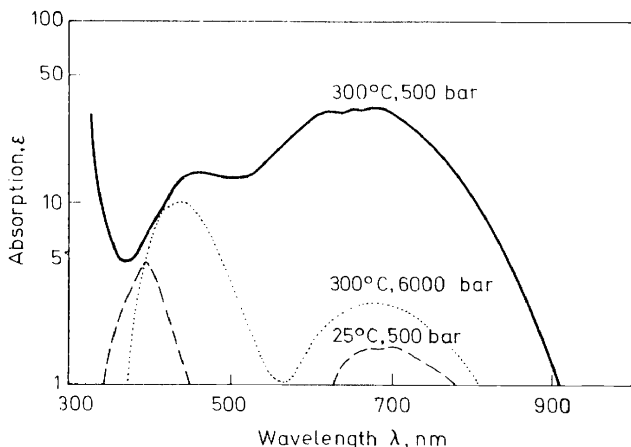


*Figure 10.* Absorption spectrum of NiCl$_2$ (Molality: 0·025) in aqueous NaCl solution (Molality: 4·0).

and at pressures between 150 and 300 bar. A detailed analysis of the magnitude of the extinction coefficients suggests that trichloromonoaquo and dichloro-diaquo tetrahedral complexes are the most abundant types. Pressures of several kilobars thus increase the range of stability of higher coordinated aquocomplexes to temperatures which may even be above the critical temperature of pure water. This is probably true also for other heavy metals of geochemical importance.

## IV. CRITICAL PROPERTIES OF AQUEOUS MIXTURES —

One-component systems have a critical point at the end of the vapour pressure curve. Two-component systems have a critical curve in the three-dimensional pressure/temperature/composition diagram. This curve may be uninterrupted or interrupted and distorted[21]. *Figure 11* gives schematically a few examples as pressure/temperature diagrams. Below, to the left, two vapour pressure curves of a low boiling and a very high boiling substance are shown with their triple points TP and critical points C. The projections of gas–liquid–solid three-phase planes connect the triple points with a quad-ruple point Q. The critical points are connected by a critical curve C, projected on the $P/T$-plane. Steeply rising melting pressure curves begin at the triple points. At the lower right an isothermal cross section at $T_a$ is shown. The maximum on the liquid–gas phase boundary curve is one point on the critical curve. Diagrams of this kind have been observed for the sodium chloride–water system[22]. In other systems the Q–TP$_2$–three phase boundary surface

21

extends to high temperatures and intersects the $C_1C_2$ critical curve at 'critical end points'. The silica–water system is an example for this behaviour[23].

Two fluid components which are not too different, as for example ethane and hexane, have a normal critical curve as in the upper left diagram of
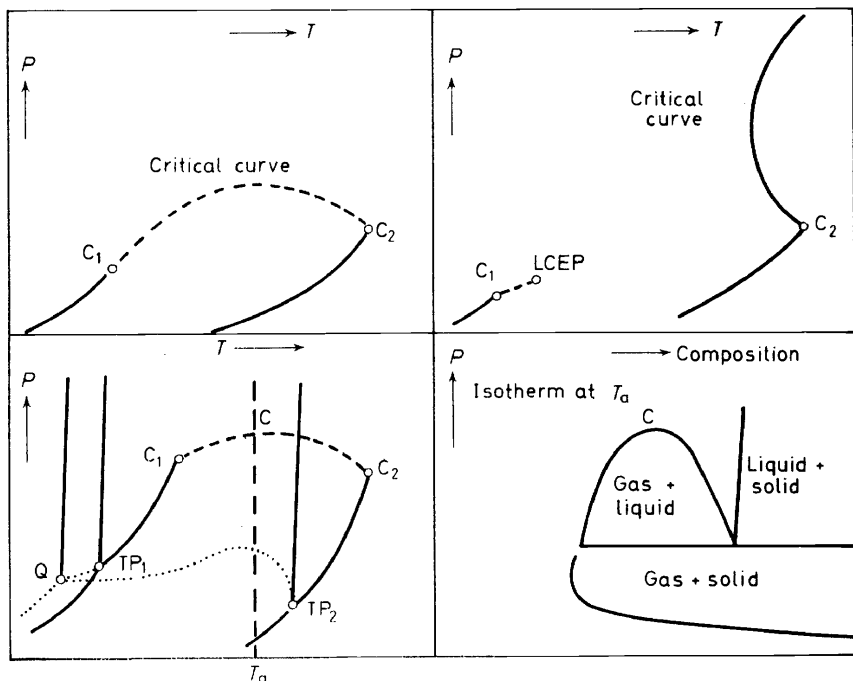


*Figure 11.* Critical curves of two-component systems.

*Figure 11.* If there is a greater difference in size, polarity, etc., the critical curve may also be interrupted at a lower critical end point (LCEP) with an upper branch as shown in the upper right diagram of *Figure 11.* This behaviour can be interpreted as an interference between a liquid–liquid miscibility range with the liquid–gas critical curve[24]. If this upper branch of the critical curve has a minimum temperature as in the diagram then the behaviour described by the critical curve at pressures higher than the pressure of this minimum temperature is sometimes called 'gas–gas-immiscibility'. It has been predicted by van der Waals and was demonstrated experimentally first by Krichevskii[25, 26] with nitrogen and ammonia in 1940. Since then, other examples have been found[24, 26] and discussed[27]. Among these are carbon dioxide–water[28], benzene–water[29], ethane–water[30] and argon–water[31]. The upper branches of the critical curves of these systems are shown in *Figure 12.*

They begin at the critical point of water and have a minimum temperature with the exception of the water–argon system. The range of complete miscibility is always on the right side, that is on the high temperature side, of these curves. One can have homogeneous mixtures of liquid-like densities at all
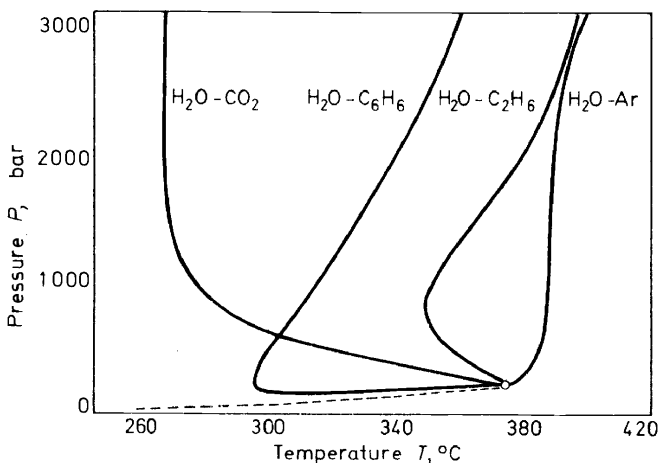
22

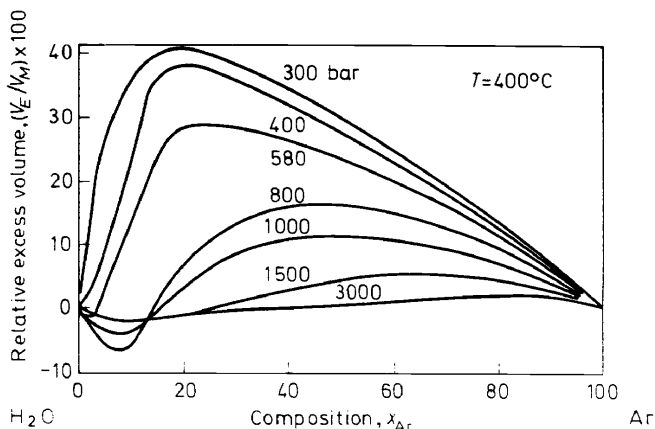*Figure 12.* Critical curves of several binary aqueous systems.



*Figure 13.* Relative excess volume $V_E/V_M$ of supercritical water–argon mixtures at pressures between 300 and 3 000 bar.

concentrations if the pressure can be raised to the order of about 2 kb at temperatures higher than the critical temperatures at these pressures. Such dense gaseous mixtures may find practical applications.

The water–argon system may also be representative for combinations of other small inert molecules with water. *Figure 13* gives an indication of the amount and character of deviation from ideal behaviour of the supercritical argon–water mixtures. The molar excess volume $V_E$ divided by the molar volume of the mixture at the respective conditions $V_M$ has been plotted for 400°C as a function of composition[31]. While the excess volume at relatively low pressure is large and positive, it reduces to a few per cent at 3 kb. The S-shaped behaviour with negative excess volumes at high water concentrations can be qualitatively explained with relatively simple models, for

23

example spheres with 'square well' interaction potentials combined with small 'hard sphere' particles[32].

## V. CONDUCTANCE OF ELECTROLYTE SOLUTIONS

From the knowledge of the dielectric constant it can be expected that dense water at high temperatures will remain a good electrolytic solvent. *Figure 14* demonstrates the effect of increased pressure on the conductance of three types of electrolytes at relatively low temperatures. Detailed discussions of these phenomena have been given elsewhere [33, 34]. In *Figure 14* the
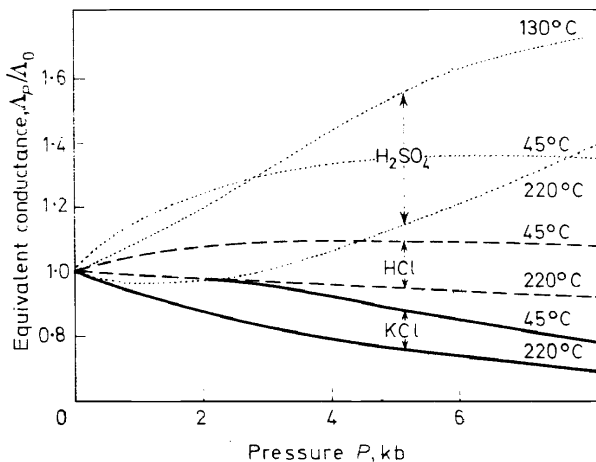


*Figure 14.* Pressure dependence of the equivalent conductance $\Lambda$ of $0.001$ M KCl, HCl and $H_2SO_4$ in water.

relative changes of the equivalent conductances with pressure are shown. For a normal strong electrolyte such as potassium chloride, pressure increase causes a decrease in conductance[35]; this is in qualitative accordance with Walden's rule, which predicts that the equivalent conductance should be proportional to the inverse of solvent viscosity. The conductance decrease of potassium chloride with pressure is smaller, however, than estimated by this rule, since the effective ionic radii are not independent of pressure. For hydrogen chloride the conductance decreases only very slightly at 220°C and increases at 45°C. This is due to the enhancement of the abnormal mobility of protons in associated water[36]. A similar effect would be observable for hydroxyl ions. The pressure dependence of the conductance of sulphuric acid, shown in *Figure 14*, can be understood as the result of the combined pressure dependences of water viscosity, abnormal proton mobility and dissociation of $HSO_4^-$-ions into protons and sulphate ions. The equilibrium constant for this dissociation has a negative temperature dependence and a positive pressure dependence[36]. At 100°C for example, the constant rises from $0.8 \times 10^{-3}$ to $48 \times 10^{-3}$ mole/l. if the pressure is increased to 8 kb. The increase of electrolytic dissociation with pressure is mainly due to the

24

fact that water molecules within the hydration spheres of the produced ions are more densely arranged than in the free fluid. This effect is particularly evident in supercritical aqueous solutions where the compressibility of the fluid is high. A number of electrolytes, simple acids, alkali hydroxides and halides have been investigated in recent years to about 700°C and 6 kb[37, 38, 39]. Maximum equivalent conductances have been observed at water densities between 0·4 and 0·8 g/cm$^3$ which are up to one order of magnitude greater than at room temperature. The conductivity of dilute aqueous potassium chloride solutions could be measured to 1000°C and 12 kb[40]. A piston-cylinder type apparatus with internal heating has been used. The electrolyte solution was compressed by a uniaxial press within a micro conductance cell which could be heated in a few minutes to the desired temperature, thus reducing contamination by corrosion. A platinum-sheathed thermocouple served as one of the conductance electrodes. Results are shown in *Figure 15*. The equivalent conductance is plotted as a function of temperature for
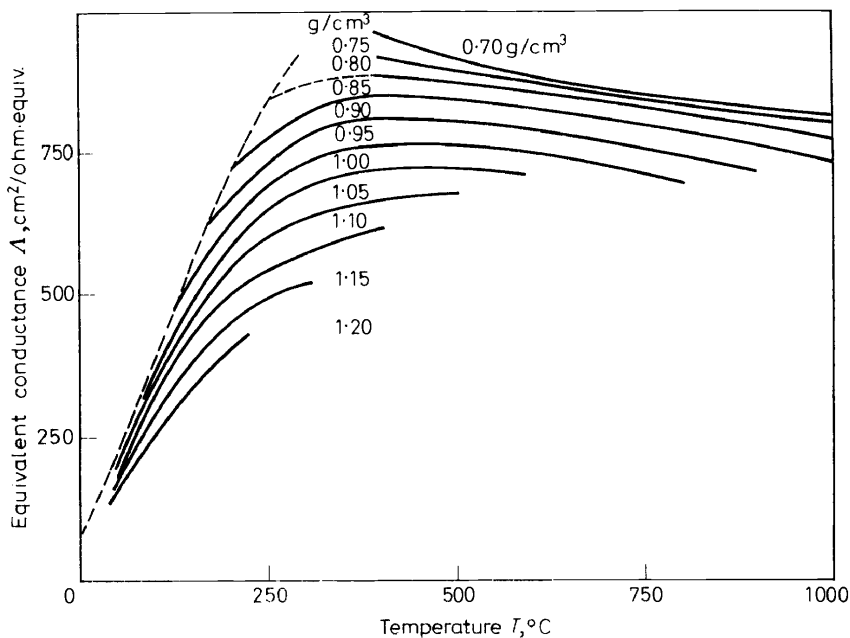


*Figure 15.* Equivalent conductance $\Lambda$ of 0·01 M KCl in water as a function of temperature at high densities. Dashed line denotes boundary of two-phase region.

different densities of the solution. Since the salt concentrations were low, the densities were assumed to be equal to the density of pure water under the same conditions. At the normal density of 1·0 g/cm$^3$, for example, the conductance increases with temperature as expected. Above 400°C, however, the curve levels off and may even have a flat maximum. The other constant density curves show similar behaviour at conductances which are seven to

25

eight times higher than at zero degrees. This phenomenon is explained by assuming ion pair formation which leads to effective degrees of dissociation of 0·7 to 0·9 at densities between 0·7 and 1·0 g/cm³ and temperatures higher than 400°C. The ion pair association constant above 400°C appears to be remarkably independent of temperature at constant density, probably because the product of dielectric constant and temperature varies only very little under these conditions[40]. Also, the viscosity does not change very much with temperature at these densities above 400°C.

## VI. IONIC DISSOCIATION OF PURE WATER

The enthalpy of the ionic dissociation of water is +13·4 kcal/mole at standard conditions. The volume decrease connected with the dissociation is −21 cm³/mole[41]. Thus a combination of temperature increase and pressure increase should produce very high values of the ion product in water. Hamann et al.[42,43] reported shock wave measurements of the electrical conductivity of water at shock pressures between 20 and 130 kb with temperatures extending to about 800°C. While the specific conductance of pure liquid water at 20°C and atmospheric pressure is $4 \times 10^{-8}$ ohm$^{-1}$ cm$^{-1}$, a value of 1·2 ohm$^{-1}$ cm$^{-1}$ was observed at 133 kb and 804°C. This increase in conductance by more than seven orders of magnitude was confirmed by static conductance measurements[44], where more combinations of pressure and temperature are possible than in the shock wave experiments. A very small amount of
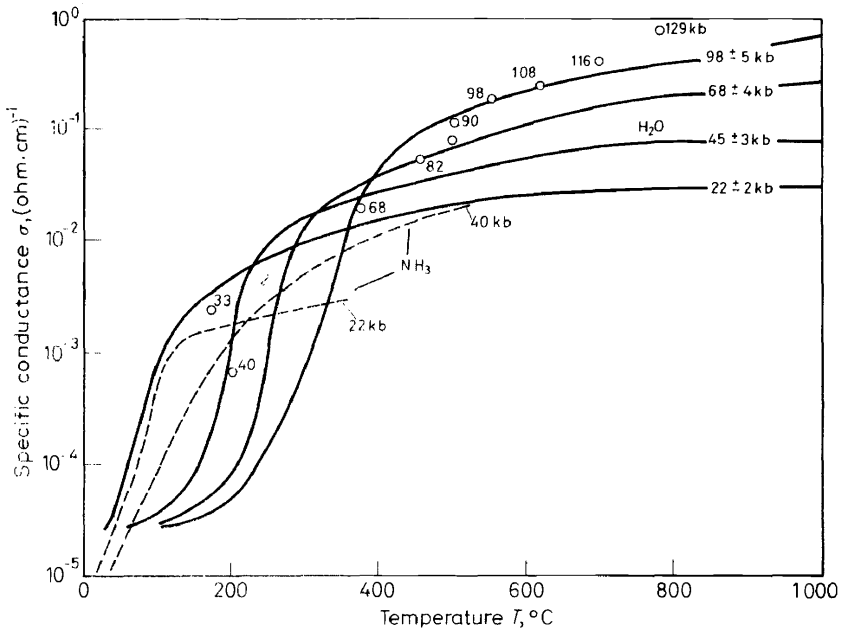


*Figure 16.* Specific conductance σ of pure water and pure ammonia at high temperatures and pressures. ○ denotes shock wave results of Hamann *et al.* The curves are results from static experiments.

26

water was filled into a platinum–iridium cell placed between two opposed tungsten carbide anvils. The water was frozen to $-30°C$, compressed to the desired pressure and then heated by graphite resistance heaters while the conductance was recorded. *Figure 16* gives isobars of the specific conductance as a function of temperature. The pressures have been calibrated by metal transition points and melting pressure curves of salts and ice. Starting from a low conductance the curves rise while the ice is melting. It is assumed that, after levelling off, that is for example above 500°C for the 98 kb isobar, the curves give the conductance of the fluid water.

The circles showing the earlier shock wave results of Hamann *et al.*[42] are consistent with the static measurements considering the difficulties and differences of the two methods. This means that water at 1000°C and pressures between 100 and 120 kb has a specific conductance comparable to to the conductance of a concentrated aqueous salt solution at 25°C.

The observed large increase of conductance is mainly due to an increase of the 'ionization product', that is of the product of the activities of hydrogen ions and hydroxyl ions in mole/l. Within the accuracy of this discussion the activities can be replaced by concentrations. It has been shown that the ion mobilities even at these extreme conditions can be relatively well estimated[45, 42] or derived from measurements with shocked salt solutions[46]. The sum of the ion mobilities for hydrogen ions and hydroxyl ions at 670°C
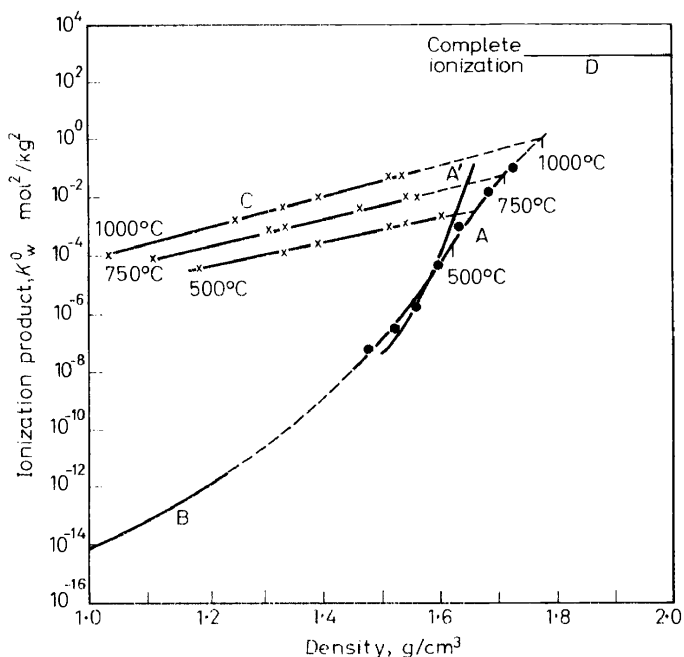


*Figure 17.* The ionization product $K_w$ of water as a function of density according to Hamann and Linton. ● denotes shock wave results of Hamann and Linton, × static measurements of Holzapfel and Franck[44].

27

and 114 kb for example should be $2090 \pm 500 \, \text{cm}^2 \, \text{ohm}^{-1} \, \text{mole}^{-1}$. *Figure 17*, which is from Hamann and Linton[46], gives the ionization product of water derived from static and shock wave experiments as a function of density for several temperatures. At 1000°C and densities between 1·5 and 1·7 g/cm³ the ionization product reaches values of $10^{-2}$ to $10^{-1} \, \text{mole}^2 \, \text{l}^{-2}$. This increase of the product by more than twelve orders of magnitude over the value for standard conditions is not unreasonable if one assumes a constant energy of dissociation and an average reaction volume change for the pressure range between 7 and 10 cm³/mole. It has been suggested that water may become an ionic fluid if compressed to densities higher than about 1·8 g/cm³ at high supercritical temperatures[46, 47]. This plausible suggestion means that water at these conditions would behave similarly to fused sodium hydroxide. It is indicated in the upper right corner of *Figure 17*.

Recently conductance measurement with pure fluid ammonia have been made to 600°C and 40 kb using a similar method as in the water experiments[48]. The two broken curves in *Figure 16* give the results. It appears as if the ionization would also be increased substantially by raising temperature and pressure. The ionization product for ammonia at 500°C and 40 kb has been estimated from these conductance data to be $4 \times 10^{-4} \, \text{mole}^2 \, \text{l}^{-2}$. This would be an increase by about a factor of about $10^{18}$ over the value for 25°C at saturation pressure[49].
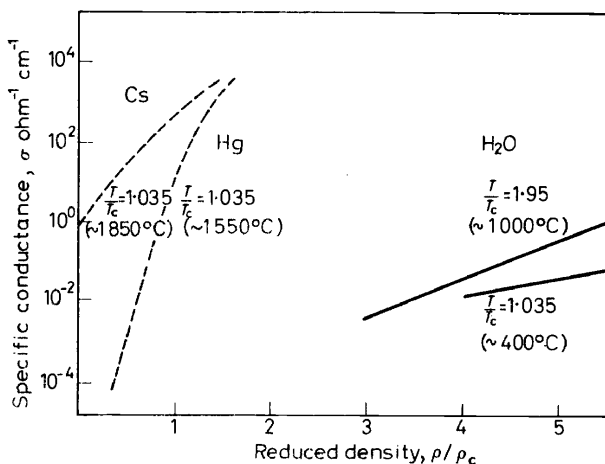


*Figure 18*. Specific conductance $\sigma$ of supercritical caesium and mercury and of supercritical water as a function of reduced density $\rho/\rho_c$

As a conclusion it may be interesting to compare the electric conductance of dense supercritical water with the conductance of dense gaseous supercritical mercury[50] and caesium[51]. This is done in *Figure 18*. The logarithm of the specific conductance is plotted as a function of reduced density. The actual density is divided by the critical density of each substance. The comparison is made at a reduced temperature of 1·035—slightly above the critical point. For water, however, a second curve for a reduced temperature

28

of almost two is given. The difference in behaviour is very obvious. Mercury and caesium already attain a conductance of 1 000 ohm$^{-1}$ cm$^{-1}$ at less than twice the critical density. This has been shown as due to electronic conductance in the dense gas phase[50]. For water, as an ionic conductor, compression to more than five times the critical density and twice the critical temperature is necessary to reach a specific conductance of 1 ohm$^{-1}$ cm$^{-1}$.

## REFERENCES

1 S. Maier and E. U. Franck, *Ber. Bunsenges. Phys. Chem.* **70**, 639 (1969).
2 H. Köster and E. U. Franck, *Ber. Bunsenges. Phys. Chem.* **73**, 716 (1969).
3 C. W. Burnham, J. R. Holloway and N. F. Davis, *Amer. J. Sci., A*, **267**, 70 (1969).
4 H. M. Rice and I. M. Walsh, *J. Chem. Phys.* **26**, 815 (1957).
5 K. H. Dudziak and E. U. Franck, *Ber. Bunsenges. Phys. Chem.* **70**, 1120 (1966).
6 E. A. Bruges and M. R. Gibson, *J. Mech. Engng Sci.* **11**, 189 (1969).
7 J. G. Kirkwood, *J. Chem. Phys.* **7**, 911 (1939).
8 D. Eisenberg and W. Kauzmann. *The Structure and Properties of Water.* Clarendon Press: Oxford (1969).
9 A. S. Quist and W. L. Marshall, *J. Phys. Chem.* **69**, 3165 (1965).
10 K. Heger, *Thesis, 1969.* Institute for Physical Chemistry, University of Karlsruhe, Germany.
11 J. A. Pople, *Proc. Roy. Soc. A.* **205**, 163 (1951).
12 E. U. Franck and K. Roth, *Disc. Faraday Soc.* **43**, 108 (1967).
13 W. F. J. Hare and H. L. Welsh, *Canad. J. Phys.* **36**, 88 (1958).
14 F. M. Buback, *Thesis, 1969.* Institute for Physical Chemistry, University of Karlstruhe, Germany.
15 H. Lindner, *Thesis, 1970.* Institute for Physical Chemistry, University of Karlsruhe, Germany.
16 G. E. Walrafen, in *Hydrogen-bonded Systems*, Taylor and Francis: London (1968).
17 H. C. Helgeson, *Amer. J. Sci.* **267**, 729 (1969).
18 H. D. Lüdemann and E. U. Franck, *Ber. Bunsenges. Phys. Chem.* **71**, 455 (1967).
19 H. D. Lüdemann and E. U. Franck, *Ber. Bunsenges. Phys. Chem.* **72**, 514 (1968).
20 D. Rykl and H. D. Lüdemann, *J. High Temp. High Press. Res.* **1**, 457 (1969).
21 J. S. Rowlinson, *Liquids and Liquid Mixtures*, 2nd ed. Butterworths: London (1969).
22 S. Sourirajan and G. C. Kennedy, *Amer. J. Sci.* **260**, 115 (1962).
23 G. C. Kennedy, G. J. Wasserburg, H. C. Heard and R. C. Newton. *Publ. No. 150*, Institute of Geophysics, UCLA (1960).
24 G. Schneider, *Ber. Bunsenges. Phys. Chem.* **70**, 497 (1966).
25 J. R. Krichevskii, *Acta Physicochimica, U.R.S.S.* **12**, 480 (1940).
26 D. S. Tsiklis, *Handbook of Techniques in High Pressure Research and Engineering*, Plenum: New York (1969).
27 J. M. Prausnitz, *Molecular Thermodynamics of Fluid Phase Equilibria.* Prentice–Hall: New York (1969).
28 K. Tödheide and E. U. Franck, *Z. Phys. Chem. (Frankfurt)*, **37**, 387 (1963).
29 Z. Alwani, *Thesis, 1969.* Institute for Physical Chemistry, University of Karlsruhe, Germany.
30 A. Danneil, K. Tödheide and E. U. Franck, *Chem-Ing-Tech.* **39**, 816 (1967).
31 H. Lentz and E. U. Franck, *Ber. Bunsenges. Phys. Chem.* **73**, 28 (1969).
32 M. Rigby, B. J. Alder, A. M. Lapse and C. E. Hecht, *J. Chem. Phys.* (1970) (in press).
33 S. D. Hamann, *Physicochemical Effects of Pressure.* Academic Press: New York (1957).
34 K. E. Weale, *Chemical Reactions at High Pressures.* Spon: London (1967).
35 F. Hensel and E. U. Franck, *Z. Naturforschung*, **19a**, 127 (1964).
36 E. U. Franck, D. Hartmann and F. Hensel, *Disc. Faraday Soc.* **39**, 200 (1965).
37 E. U. Franck, *Angew. Chem.* **73**, 309 (1961).
38 G. Ritzert and E. U. Franck, *Ber. Bunsenges. Phys. Chem.* **72**, 798 (1968).
39 W. L. Marshall, *Rev. Pure Appl. Chem.* **18**, 167 (1968).
40 K. Mangold and E. U. Franck, *Ber. Bunsenges. Phys. Chem.* **73**, 21 (1969).
41 S. D. Hamann, *J. Phys. Chem.* **67**, 2233 (1963).
42 H. G. David and S. D. Hamann, *Trans. Faraday Soc.* **55**, 72 (1959); **56**, 1043 (1960).
43 S. D. Hamann and S. D. Linton, *Trans. Faraday Soc.* **62**, 2234 (1966).
44 W. Holzapfel and E. U. Franck, *Ber. Bunsenges. Phys. Chem.* **70**, 1105 (1966).

[45] W. Holzapfel, *J. Chem. Phys.* **50**, 4424 (1969).

[46] S. D. Hamann and M. Linton, *Trans. Faraday Soc.* **65**, 2186 (1969).

[47] S. D. Hamann and M. Linton, paper presented at the XXIInd International Congress of Pure and Applied Chemistry, Sydney, Australia, 20–27 August 1969.

[48] D. Severin, *Thesis, 1969.* Institute for Physical Chemistry, University of Karlsruhe, Germany.

[49] L. V. Coulter, J. R. Sinclair, A. G. Cole and G. C. Roper, *J. Phys. Chem.* **81**, 2986 (1959).

[50] F. Hensel and E. U. Franck, *Rev. Mod. Phys.* **40**, 697 (1968).

[51] H. Renkert, F. Hensel and E. U. Franck, *Physics Letters*, **30A**, 494 (1969).